Thermal, Morphological, and X-ray Study of Polymer-Clay Nanocomposites

Vineeta Nigam,[1] Hitesh Soni,[2] Madhumita Saroop,[2] G.L. Verma,[2] A.S. Bhattacharya,[3] D.K. Setua[1]

[1]*Defence Materials & Stores Research & Development Establishment, DMSRDE Post Office, G.T. Road, Kanpur 208013, India*
[2]*Delhi Technical University, Bawana Road, Delhi 110042, India*
[3]*Auropol India Pvt. Ltd. 40A, C.R. Avenue, Kolkata, India*

Received 23 November 2009; accepted 23 May 2011
DOI 10.1002/app.34956
Published online 14 November 2011 in Wiley Online Library (wileyonlinelibrary.com).

ABSTRACT: Synthesis and characterization of polymer nanocomposites consisting of diglycidyl ether of bisphenol-A with inorganic as well as organically modified nanosized clay fillers, for example, vermiculites and montmorillonite, obtained from trade, are studied. Confirmations of intercalation and exfoliation characteristics of these fillers into the cured epoxy resin matrix have been investigated by wide angle X-ray diffraction studies. Scanning electron microscopy and atomic force microscopy techniques have been adopted to assess the nature of filler dispersion, size of the agglomerates, and the polymer-filler adhesion. While significant improvement in the mechanical properties (i.e., tensile, flexural strength, and modulus) has been observed, the thermo-oxidative stability of the composites measured by thermogravimetric analysis showed only marginal improvement. © 2011 Wiley Periodicals, Inc. J Appl Polym Sci 124: 3236–3244, 2012

Key words: polymer-clay nanocomposite; vermiculite; montmorillonite; SEM; AFM; DGEBA

INTRODUCTION

Montmorillonites (MMTs) have beginning to be used in polymers because of their high aspect ratio, presence of a 2 : 1 layered structure ($\sim$ 1 nm in thickness, with layer spacing ranging from 0.98 to 1.8 nm) and scope of formation of platelets, 30–50 nm in lateral dimensions, if properly exfoliated.[1–5] Characteristic features of MMT also include their ability to absorb certain cations which are mostly exchanged by other cations, for example, Na^+, Ca^{2+}, Mg^{2+}, H^+, K^+, and NH_4^+ in a water solution. Different types of polymers used in association with MMT for development of nanocomposites are polystyrene,[6] poly (*N*-vinylcarbazole),[7] and epoxy resins.[8–12] Studies on phase morphology, mechanical, and viscoelastic properties of exfoliated epoxy/MMT nanocomposite have been reported.[13,14] Pelissou et al.[15] have described the electrical and thermal characterization of nanocomposites consisting of an epoxy matrix containing micrometric quartz and small amount of nanoclay. Published literature also gives description of use of nanoclay as filler in polyaniline, polymethylmethacrylate, and polyurethanes for different applications.[16–19] Powell and Beall[20] have reported on the physical properties of polymer/clay nanocomposites. Sharon et al.[21] have prepared nanocomposites using Cloisite 30B and diglycidyl ether of bisphenol-F and diaminodiphenyl sulfone and investigated relationship between extent of exfoliation and mechanical properties.

Likewise MMT, vermiculite (VMT) also possesses a 2 : 1 layered structure where one octahedral sheet is sandwiched between two opposing tetrahedral sheets resulting in a layer spacing between 1.0 and 1.5 nm. Due to isomorphic substitutions in the lattice, the layers have permanent negative charges that are compensated by hydrated Mg^{+2} or K^+ cations in the interlayer space. VMT has been used with polypropylene[22–26] and oligothiophene,[27] essentially for better functional properties. Nisha et al.[28] have carried out synthesis of VMT filled poly (4-vinylpyridine) and their characterization by spectroscopic techniques. Patro et al.[29] have reported on the structure of polyurethane-VMT nanocomposite foams. Zhang et al.[30] have prepared polyamide 6, 6/organo-VMT (OVMT) nanocomposites via melt mixing using varied concentrations of premodified and exfoliated OVMT. Valle et al.[31] have carried out synthesis of nanocomposites by *in situ* oxidative polymerization of pyrrole in the interlayer spaces of VMTs. Tang et al.[32] have reported on thermal stabilities of a series of VMT/polystyrene nanocomposites. Epoxy nanocomposites with organically modified VMT (by ammonium ions) synthesized using a solution casting approach for better oxygen and

Correspondence to: D.K. Setua (dksetua@rediffmail.com).

TABLE I
Material Properties of MMT and VMT

S.no.	Property	Montmorillonite K-10[a]	Vermiculite dupre fine grade[b]
1	CEC (meq/gm)	80–150	100–150
2	Sp. surface area	700–800	500–700
3	Basal spacing (nm)	0.98–1.8+	1.0–1.5+
4	Sp. Gravity	2.3–3.0	2.5
5	Average particle size	5 μ	10 μ
6	Physical form	White powder	Brown flakes
7	Crystalline structure	Monoclinic	Platy crystals

[a] Chemical formula of Montmorillonite K-10 {(Na,Ca) $(Al,Mg)_6(Si_4O_{10})_3.(OH)_6nH_2O$}.
[b] Chemical formula of Vermiculite Dupre Fine grade {$(Mg,Fe{+}{+},Al)_3(Al,Si)_4O_{10}(OH)_24(H_2O)$}.

water vapor permeation properties compared with montmorillonite, modified with the same ammonium ions, have been reported by Mittal.[33]

The *in situ* polymerization technique has been found to be most effective in the preparation of a variety of thermoset polymer matrix nanocomposites. Intercalated nanocomposites are formed when there is limited inclusion of polymer chain between the clay layers with a corresponding small increase in the interlayer spacing of few nanometers, whereas exfoliated structures are formed when the clay layers are well separated from one another and are individually dispersed in the continuous polymer matrix.[34] In this work, we report our studies on thermal, morphological, wide angle X-ray diffraction (WAXS), dynamic mechanical, and impact strength of MMT- and VMT-based epoxy nanocomposites.

EXPERIMENTAL

Materials

Industrially purified MMT (K-10 grade) and octadecylamine were obtained from ς-Aldrich, Switzerland. The epoxy resin (diglycidyl ether of bisphenol-A, DGEBA) and the aromatic curing agent [diamino diphenyl mathane (DDM)] were procured from Ciba-Geigy, Mumbai, India. VMT (Dupre DL grade of magnesium aluminum silicate) was obtained from Minelco Specialities, UK. The material properties of these clays are summarized in Table I.

Preparation of organically modified MMT and VMT

Fifteen grams of clay was dispersed in 1200 mL of distilled water. Octadecyl ammonium chloride solution was prepared by mixing octadecylamine (5.66 g) with 2.1 mL HCl (10*N*) in 300 mL water and poured into the clay-water mixture at 80°C and stirred for 1 h. The mixture was then filtered and washed with 50/50 vol % ethyl alcohol and water mixture until no chloride was detected in the mother liquor. The octadecylamine-modified fillers (e.g., OMMT or OVMT) were subsequently dried in vacuum oven at 75°C for 3–4 days and stored in a desiccator.

Preparation of nanocomposites

Formulations of the mixes are given in Table II. DGEBA was mixed with either OMMT or OVMT in varied proportions of 0, 1.5, 3.0, 4.5, and 6.0 wt %, swelled for 3 h at 75°C and a stoichiometric amount of DDM (27 g) was added. The mixture was then out-gassed in a vacuum oven, poured into a steel mold preheated at 75°C and cured for 3 h at 75°C followed by post curing for 12 h at 110°C. For comparison, unmodified filler (MMT/VMT) with either 3 or 6 wt %, as such, were used to prepare samples following the same procedure.

Characterization of nanocomposites

Differential scanning calorimetric (DSC) studies were carried out in DSC (Model 2910, TA Instruments, DE) and TGA 2950 (also of TA Instruments) was used for thermo gravimetric analysis. Both experiments were conducted at a heating rate of 20°C/min in nitrogen atmosphere. Carl Zeiss Supra 55VP scanning electron microscopy (SEM) was used for microscopic analysis in backscatter electron mode. Explorer model atomic force microscopy (AFM) of Veeco Instruments, Singapore with silicon nitride tips and integrated cantilevers of spring constant of 0.38 Nm^{-1} was used for AFM imaging. A resolution of 256 × 256 pixels for data acquisition in the noncontact mode was employed with frequency of cantilever of 275 Hz, scan rate of 0.5–0.78 Hz and x–y scan size from 7.86 × 7.86−10 × 10 μm. The interlayer distance and diffraction pattern of nanocomposites using small angle X-ray scattering (SAXS) studies was carried out on H3 Micro model of Hecus Company from Austria. At room temperature, the 2θ scan was set at 0 to 5^0 with tungsten

TABLE II
Formulation of the Epoxy-Clay Compositions

S. no.	Epoxy resin (g)	OMMT/OVMT (g)	DDM (g)
1	100	0/0	27
2	100	1.5/1.5	27
3	100	3.0/3.0	27
4	100	4.5/4.5	27
5	100	6.0/6.0	27
S. no.	Epoxy resin (g)	MMT/VMT (g)	DDM (g)
6	100	3.0/3.0	27
7	100	6.0/6.0	27

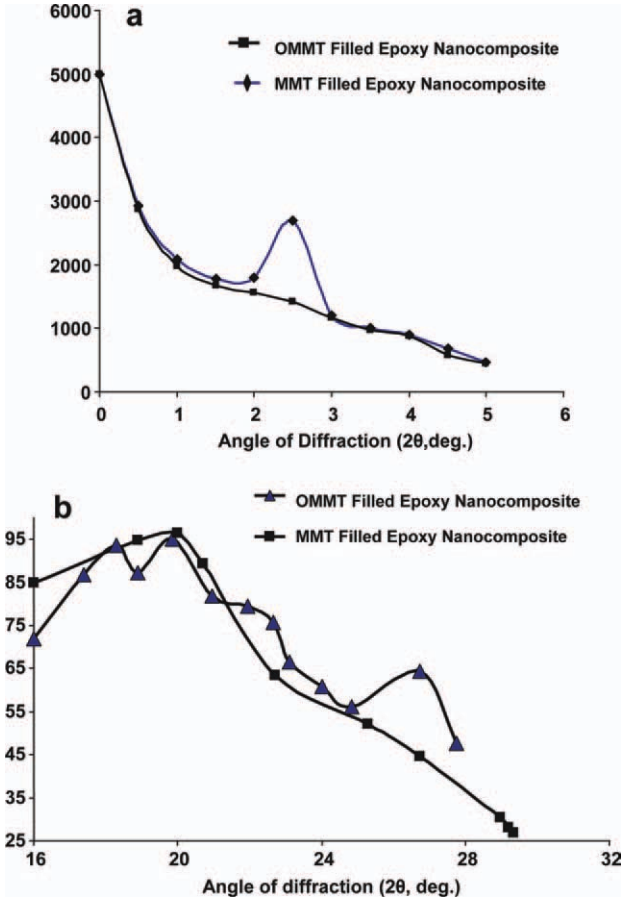

Figure 1 (a) SAXS plots of MMT and OVMT field epoxy-nanocomposites. (b) WAXS Plots of MMT and OVMT field epoxy-nanocomposites. [Color figure can be viewed in the online issue, which is available at wileyonlinelibrary.com]

filter and CuKα (λ = 1.54 E) was used as X-ray source with acceleration voltage of 40 kV and current of 30 mA. WAXS patterns of the composites were recorded in a Siefert Iso-Debye.ex-2002 diffractometer, UK with a Cu X-ray tube operating at a voltage 40 kV and current 40 mA. The instrument was configured to scan over a range of 2θ = 16° −30° at a scan rate of 0.020° (2θ) per sec.

RESULTS AND DISCUSSION

The SAXS plots of nanocomposites of epoxy resin containing suspensions of unmodified (MMT) and organically modified (OMMT) montmorillonite filler are shown in Figure 1(a). The presence of an X-ray peak at 2θ = 2.5° in case of OMMT composite indicates the presence of residual electrostatic forces. Prepolymer of the epoxy resin or its subsequent curing for generation of nanocomposites were unable to completely delaminate the montmorillonite platelets. However, moderate enhancement of the basal spacing after curing conforming to actual intercalation pushing apart the platelets from their galleries are evident from the WAXS diffractogram Figure 1(b) of the same system. Extent of increase of interlayer spacing with organic modification applicable to both MMT and VMT are given in Table III. The increase justifies occupation of the long chain alkylammonium ions dangling between the clay galleries due to poor compatibility with the epoxy matrix. However, they could catalyze the epoxy ring opening polymerization in between the silicate layers and resulted in further separation of the clay layers but not to formation of fully exfoliated structure. Owing to the dependency of the peak intensity evident in X-ray diffractograms on sample preparation or may be due to mineral defects, the analysis of the microstructure for the composites containing either OMMT or OVMT were also performed by SEM, reported later.

TABLE III
WAXS Results of MMT/VMT and OMMT/OVMT-Filled Nanocomposites

MMT	OMMT	VMT	OVMT
7.07Å (2θ = 12.50°)	14.72 Å (2θ = 5.99°)	12.55Å (2θ = 7.035°)	17.50Å (2θ = 4.96°)

The DSC studies showed that an increase of the organoclay (OMMT or OVMT) content causes a shift in the exothermal peak temperature to lower values Table IV and Table V and Figure 2(a,b). This is due to, as mentioned earlier, the catalytic effect of the octadecylammonium ions on epoxy ring opening polymerization which also leads to a decrease in the ultimate heat of reaction (ΔH). In case of OVMT, the relative changes of ΔH is higher than OMMT (compare Table IV and V). Further, a marginal decrease of *Tg* with increasing concentration of either of OMMT or OVMT signifies an absence of absorbed polymer layer on surfaces of clay particles, which

TABLE IV
Summary of the DSC Results for Epoxy-MMT Nanocomposites

S. no.	Sample designation	T_{onset} (°C)	$T_{midpoint}$ (°C)	T_{end} (°C)	T_g (°C)	Heat of reaction (ΔH, J/g)
1	1.5% OMMT	93	163.31	261.5	161.31	362.0
2	3.0% OMMT	89	161.78	256.8	159.78	353.8
3	4.5% OMMT	86	152.32	253.7	150.32	352.4
4	6.0% OMMT	83	148.39	249.9	146.39	311.8
5	3.0% MMT	87	160.99	255.6	158.99	354.2
6	6.0% MMT	89	160.89	259.9	157.89	371.0

TABLE V
Summary of the DSC Results for Epoxy-VMT Nanocomposites

S. no.	Sample designation	T_{onset} (°C)	$T_{midpoint}$ (°C)	T_{end} (°C)	T_g (°C)	Heat of reaction (ΔH, J/g)
1	1.5% OVMT	94.5	161.62	258.6	149.62	773.4
2	3.0% OVMT	90.4	161.58	256.2	149.58	771.5
3	4.5% OVMT	87.6	161.52	253.4	149.52	733.5
4	6.0% OVMT	83.9	160.11	251.7	148.11	725.9
5	3.0% VMT	88.4	161.76	251.6	149.76	351.0
6	6.0% VMT	91.2	155.25	246.5	152.25	359.2

usually increases the *Tg*. Rather, the polymer chains are tied through the surface of the silicate layers by electrostatic interaction thus reducing the surrounding entanglements. Addition of unmodified MMT or VMT on *Tg* of the composites are, however, insignificant.

Thermal stability of the nanocomposites was studied using thermogravimetric analysis and the thermograms [Fig. 3 (a,b)] showed an initial weight loss due to desorption of water, which includes interlayer, interparticulate, and constituent water from fillers. The organic constituent associated with the fillers OMMT or OVMT decomposed around 280°C and resulted in weight losses which are not present in MMT or VMT. The thermal stability of the composite containing unmodified filler is, therefore, more than that of the organomodified OMMT/OVMT nanocomposites at the same clay content.

Dynamic mechanical analysis is commonly used for studying the viscoelastic behavior of polymeric materials. It is also the preferred method for measuring the glass transition temperature (*Tg*), particularly for polymers with rigid backbone. The temperature dependence of the storage modulus for the neat and epoxy -OMMT/OVMT nanocomposites shows that below *Tg*, 3 wt % nanocomposite exhibit highest storage modulus than the neat polymer [Fig. 4(a)]. However, the unmodified filler always show higher storage modulus because of absence of plasticization effect due to organic chains of the organomodified fillers. The decrease of *Tg* of OMMT

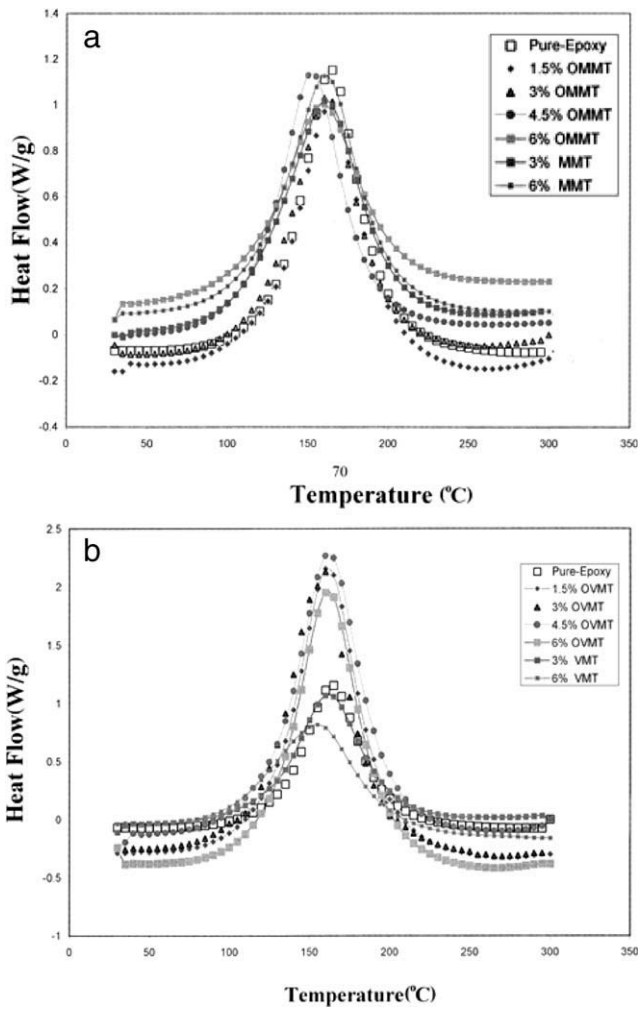

Figure 2 DSC of (a) OMMT/MMT and (b) OVMT/VMT nanocomposites.

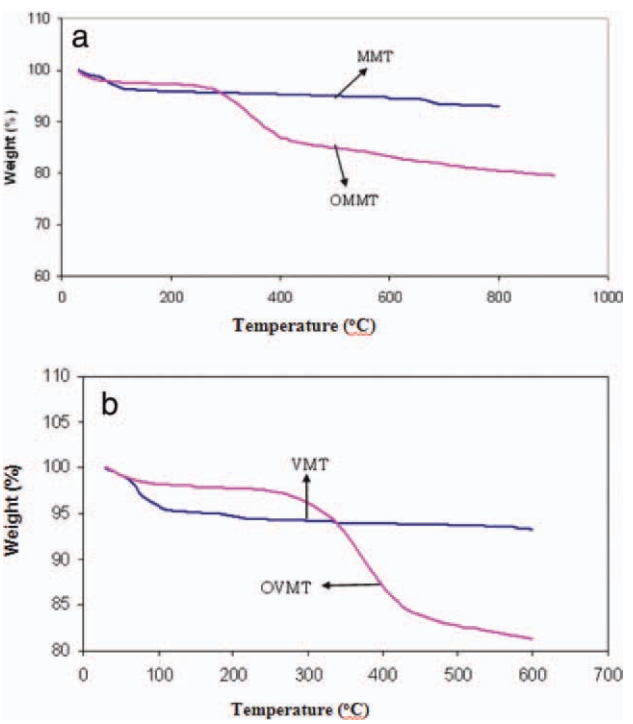

Figure 3 Comparative thermal stability of (a) MMT/OMMT nanocomposite, (b) VMT/OVMT nanocomposite. [Color figure can be viewed in the online issue, which is available at wileyonlinelibrary.com]

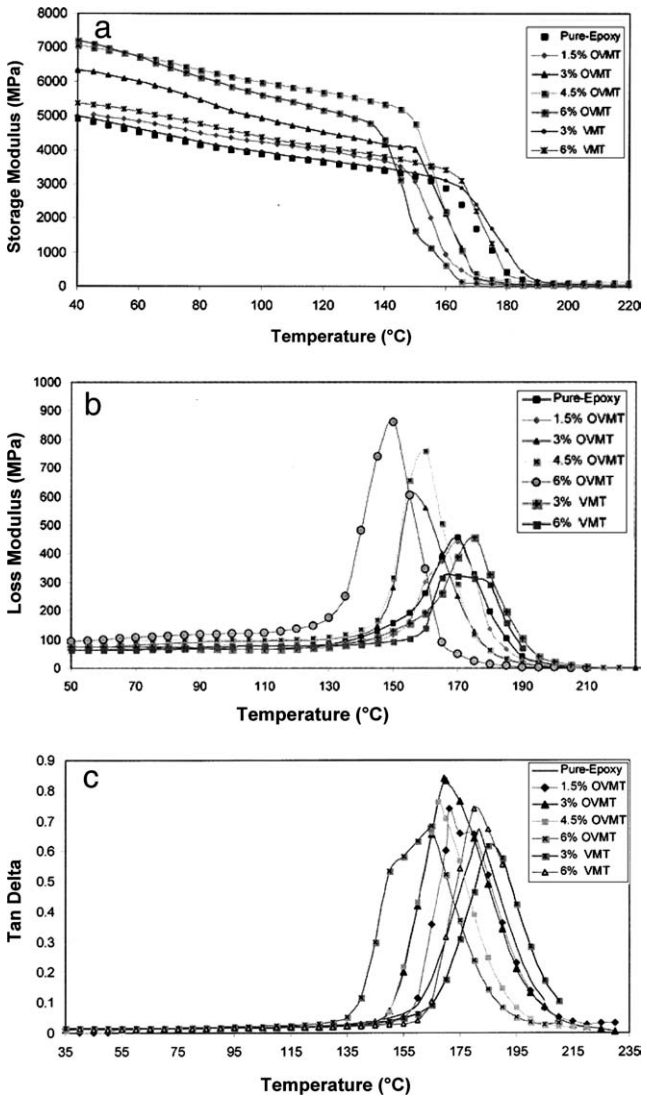

Figure 4 Dynamic mechanical analysis of OVMT-epoxy nanocomposites (a)storage modulus versus temp., (b) loss modulus versus temp. and (c)Tan delta versus temp.

and OVMT are, therefore, in conformity with our earlier observations of DSC analysis and both the storage modulus and loss modulus properties of unmodified and organically modified OMMT and OVMT nanocomposites are generally similar [Fig. 4 (a,b)]. The tan δ versus temperature plots of unmodified and organically modified OVMT nanocomposites are depicted in Figure 4(c).The peak maximum has been found at 3 wt % concentration of OVMT. The maximum *Tg* increase in case of 3% modified nanocomposite at 178°C is presumably due to proper dispersion and adequate polymer-filler interaction as inferred earlier from the X-ray diffraction data (Table III).

Mechanical properties, for example, tensile strength; tensile modulus and elongation at break and flexural strength; flexural modulus values are given in Figures 5(a–c) and 6(a,b) respectively. A rise in concentration of OMMT or OVMT results in almost 200% enhancement of tensile modulus and ultimate tensile strength, but with a sharp decrease in the elongation at breaks values. In comparison with OMMT, the OVMT filled nanocomposites show

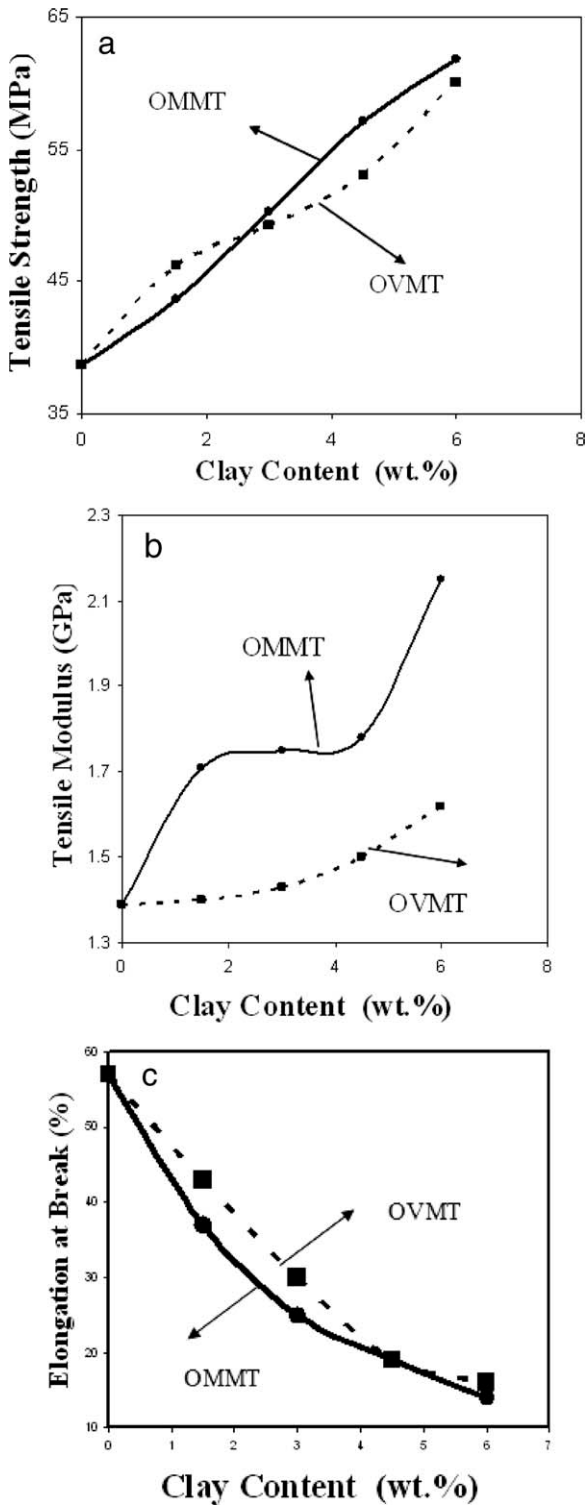

Figure 5 Mechanical properties of OMMT/OVMT-epoxy nanocomposites (a) tensile strength versus filler conc., (b) tensile modulus versus filler conc., and (c) elongation at break versus filler conc.

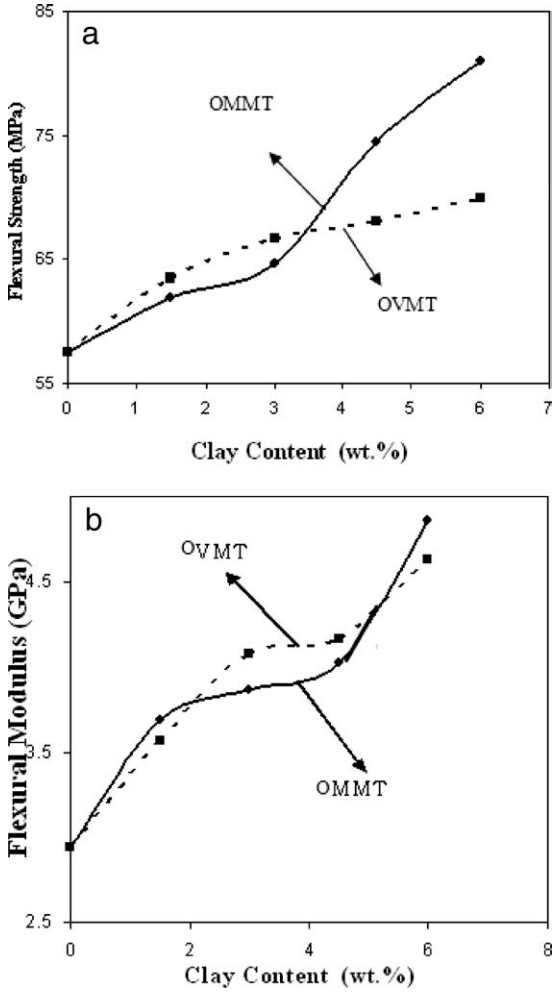

Figure 6 Flexural properties of OMMT/OVMT-epoxy nanocomposites (a) flexural strength versus filler conc., (b) flexural modulus versus filler conc.

lower tensile modulus, comparable ultimate tensile strength but higher elongation at break for 3 to 5 wt % of the filler. Similar observation has been reported earlier by others[35,36] and is generally attributed to inhomogeneous dispersion of the nanoparticles, considered as a flaw, and the strength of nanocomposite is very sensitive to the presence of these flaws. The flexural modulus of OVMT filled nanocomposites is similar to that of OMMT, but the flexural strength is lower. Besides, in case of polymer nanocomposites, there is an optimum filler concentration for best match of mechanical properties which occurs in the range between 3 and 5 wt % of filler loading.[19,37–39] In Figures 5(b) and 6(b), a plateau in both tensile modulus and flexural modulus is observed especially for the epoxy nanocomposite samples with OMMT. These are due to occurrence of quasistatic fracture toughness phenomenon valid over small variation of nano filler content between 2 and 5 wt %.[40,41] In a recent review, Kroshefsky et.al.[42] have described on the role of nanofillers in polymer nanocomposites with similarity of basic principles used in polymer blend compatibilization where a compatibilizer, either a block or a graft copolymer is commonly used in small concentration(<5 wt %). Their conclusion justifies our observation in Figures 5(b) and 6(b). It also appears that the quasistatic fracture toughness was less sensitive to clay agglomeration than the impact fracture properties as discussed in following section.

The impact strength versus varied concentration of OMMT and OVMT in the nanocomposites is shown in Figure 7. It shows an increase of impact strength up to 3% of either of the fillers followed by a decrease with increasing filler concentration. The maximum increase for OMMT (58%) is also more than OVMT (29%). The enhancement of impact strength up to 3% of OVMT or OMMT is due to combined effect of retention of nanostructure of the fillers with less agglomeration and their homogeneous dispersion in the matrix resin. These resulted in lower hardness and higher flexibility of the composites at lower filler concentration, facilitating better impact strength and an optimum value at 3–5 wt % filler loading.

SEM photomicrographs of impact failed surfaces of epoxy resin containing either 3 wt % of OMMT or OVMT are shown in Figures 8(a–c) and 9(a–c), respectively. Figure 8(a), the fractured surface of OMMT filled nanocomposite, shows that the filler particles have very good polymer-filler adhesion which is further confirmed by a magnified view of the sample shown in Figure 8(b). The presence of tiny shear lips generated across the perimeter surface of the filler agglomerates and their intermittent termination at a short distance in the matrix itself signify absorption of the impact stress by adequate energy dissipation. Thereby, toughening of the otherwise brittle epoxy resin occurs. At higher magnification, in Figures 8(b,c), formation of tortuous tear

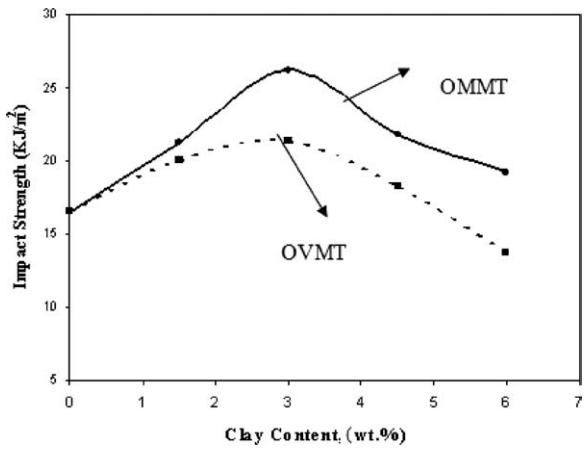

Figure 7 Impact strength versus filler conc. of OMMT/OVMT-epoxy nanocomposites.

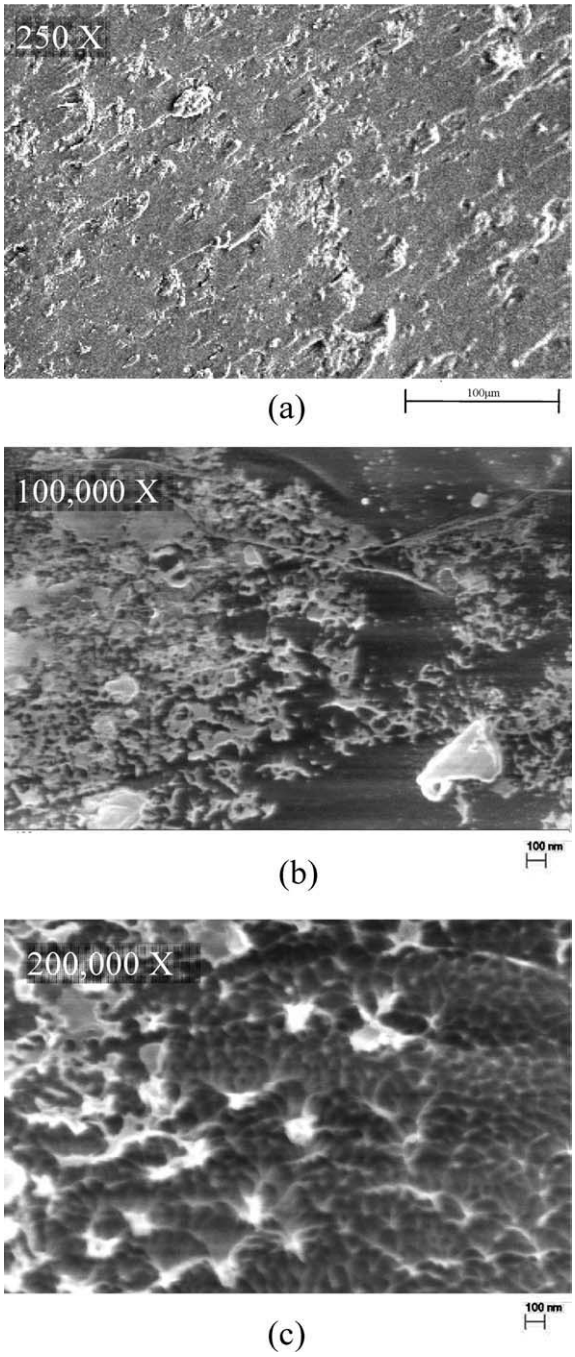

Figure 8 SEM micrograph of 3% OMMT-epoxy nanocomposite (a) 250×, (b) 100,000×, (c) 200,000×.

paths, microcracks due to detachment of some filler particles from the matrix by the impact force are also observed. The possibility of improvement of fracture toughness beyond 3 wt % of nanofillers seems to be less due to effect of agglomeration of nanoparticles and reduce flexibility of the composites with increasing filler concentration. In case of OVMT filled nanocomposite [Fig. 9(a)], we observed more brittleness, extended fracture paths and elongated shear lips compared to OMMT filled composite. The extent of filler-matrix adhesion is more than in case of OMMT [Fig. 9(b)], but there are also more agglomeration of filler particles coupled with formation of deeper grooves due to more brittle nature of the OVMT field composite [Fig. 9(c)] than OMMT. The SEM observations, summarized above, justify superior impact strength of OMMT than OVMT filled nanocomposites.

AFM imaging was conducted in noncontact mode. Both OVMT and OMMT filled nanocomposites show homogeneous filler dispersion in the nanoscale with occasional presence of agglomerates and very good

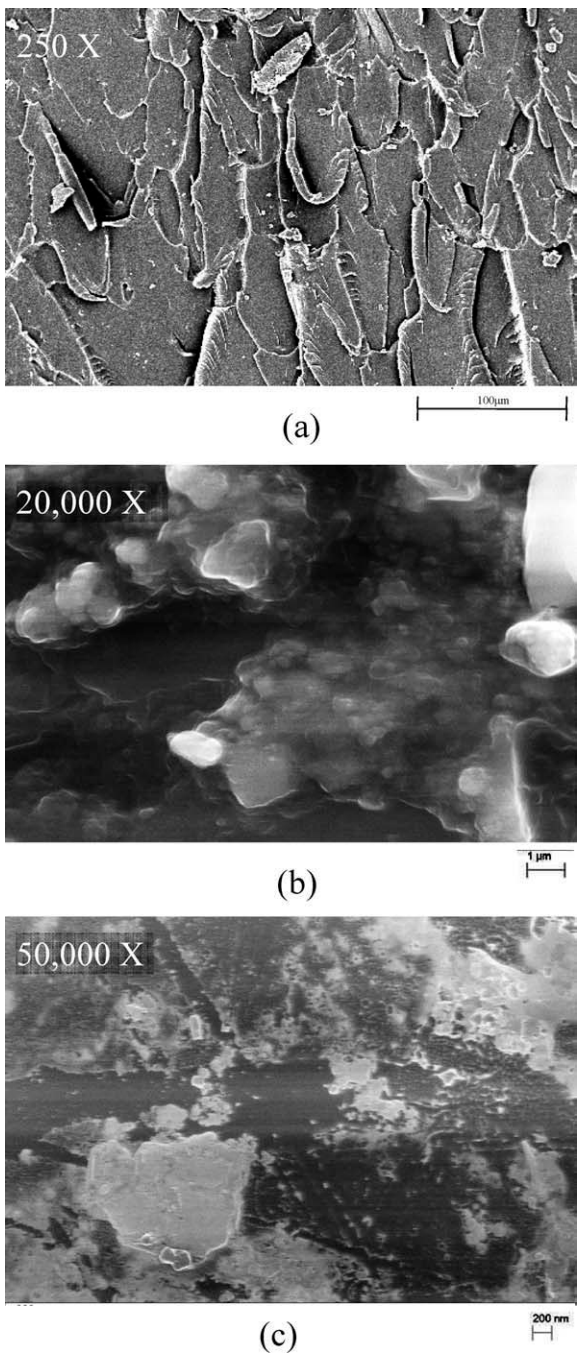

Figure 9 SEM micrograph of 3%OVMT-epoxy nanocomposite (a) 250×, (b) 20,000×, (c) 50,000×.

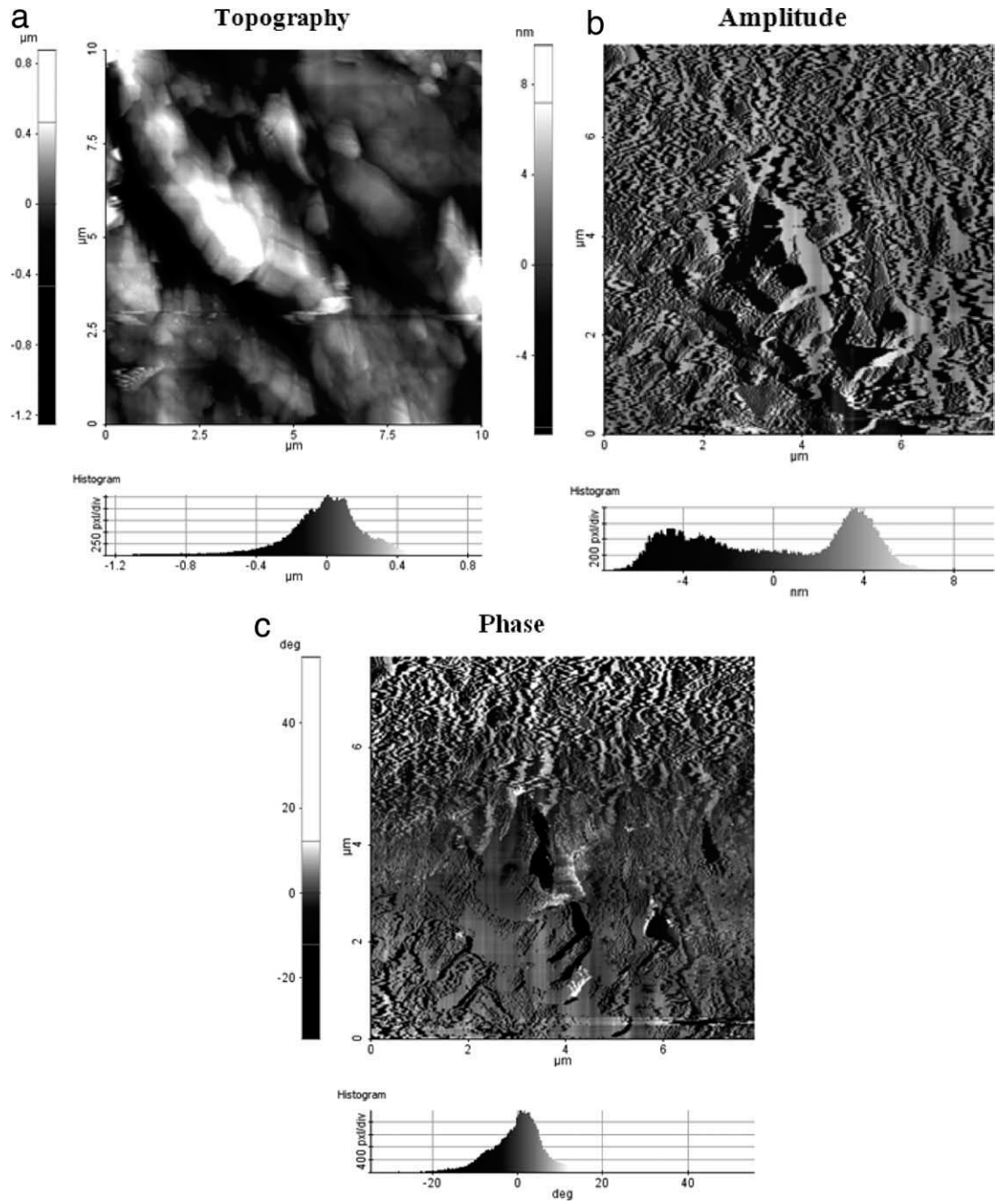

Figure 10 AFM image of 3%OMMT-epoxy nanocomposite (a) topography, histogram, (b) amplitude, histogram, (c) phase, histogram.

filler-matrix adhesion. A representative photograph of OMMT filled epoxy nanocomposite is given in Figure 10(a–c) in various modes viz., topography, phase, and amplitude. AFM observations support phase morphology obtained by SEM and corroborate the trend of mechanical properties of the nanocomposites.

CONCLUSIONS

1. Both VMT and montmorillonite, with suitable organic modification, have been found to be effective as nanofiller for the preparation of epoxy nanocomposites.
2. Octadecyl ammonium ion exchanged MMT or VMT undergo intercalation and moderate exfoliation during curing of DGEBA with DDM. The nanosize of the fillers is also retained in the cured matrix resin.
3. Thermal stability of the nanocomposites is improved by addition of organomodified MMT and VMT into epoxy resin and the extent of improvement is similar for both the fillers. However, the mechanical properties

experiences higher improvement by addition of OMMT than OVMT.
4. Damping factor or tan δ as well as Impact strength of the nanocomposites have been found to be maximum at a 3 wt % filler concentration.
5. Morphological analysis by SEM and AFM reveal homogeneous filler dispersion due to organic modification of MMT/VMT and, in effect, support the enhancement of mechanical properties of the nanocomposites.

The authors thank Dr. K. U. Bhasker Rao, Director, DMSRDE, for his suggestion and permission for publication of this work and Mr. Amit Singh, Sc 'B', for his experimental support in AFM analysis.

References

1. Vala, R. A.; Jandt, K. D.; Kramer, E. J.; Giannelis, E. P. Macromol 1995, 28, 8080.
2. Akelah, A.; Salahuddin, N.; Hiltner, A.; Baer, E.; Moet, A. Nanostruct Mater 1994, 220, 365.
3. Pinnavaia, T. J. Science 1983, 220, 365.
4. Mehrotra, V.; Giannelis, E. P. Mater Res Soc Symp Proc 1990, 171, 39.
5. Alexandre, M.; Dubois, P. Mater Sci Eng 2000, 28, 1.
6. Krishnamoorthy, R.; Vaia, R. A.; Giannelis, E. P. Chem Mater 1996, 8, 2628.
7. Biswas, M.; Ray, S. S. Polymer 1998, 39, 25.
8. Nigam, V.; Setua, D. K.; Mathur, G. N.; Kar, K. K. J Appl Polym Sci 2004, 93, 2201.
9. Ole, B.; Simon, G. P.; Varley, R. J.; Halley, P. J. Poly Eng Sci 2003, 43, 850.
10. Kormann, X.; Lindberg, H.; Berglund, L. A Polymer 2001, 42, 4493.
11. Kormann, X.; Lindberg, H.; Berglund, L. A. Polymer 2001, 42, 1303.
12. Chen, K. H.; Yang, S. M. J Appl Polym Sci 2002, 86, 414.
13. Boukerrou, A. J Appl Polym Sci 2007, 103, 3547.
14. Chin, I. J.; Thurn-Albert, T.; Kim, H. C.; Rusell, T. P.; Wang, J. Polymer 2001, 42, 5947.
15. Pelissou, S.; Besner, S.; Frechette, M.; Cole, K. C.; Desgagnes, D. IEEE Conf., 15–18 Oct. 2006, 338–340.
16. Gintert, M.; Jana, S. C.; Miller, S. Polymer 2007, 48, 4166.
17. Jimenez, G.; Jana, S. C. Compos Part A Appl Sci 2007, 38, 983.
18. Jung, C. D.; Gunes, I. S.; Jana, S. C. Ind Eng Chem Res 2007, 46, 2413.
19. Cao, F.; Jana, S. C. Polymer 2007, 48, 3790.
20. Powell, C. E.; Beall, G. W. Curr Opin Solid ST M Sci 2006, 43, 109.
21. Sharon, E. I.; John, J. L.; Richard, A. P. Polym Int 2007, 56, 1029.
22. Lan, T.; Kaviratna, P. D.; Pinnavaia, T. J Chem Mater 1995, 7, 2144.
23. Wang, Z.; Pinnavaia, T. J. Chem Mater 1998, 10, 1820.
24. Tjong, S. C; Meng, Y. Z.; Hay, A. S. Chem Mater 2002, 14, 44.
25. Tjong, S. C.; Meng, Xu, Y. J Polym Sci Part B: Polym Phys 2002, 40, 2860.
26. Tjong, S. C.; Meng, Y. Z.; Xu, Y. J Appl Polym Sci 2002, 86, 2330.
27. Ibrahim, M. A.; Lee, B. G.; Park, N. G. Synth Met 1999, 105, 35.
28. Nisha, A.; Dhamodharan, R.; Rajeshwari, M. K. J Appl Polym Sci, 2000, 76, 1825.
29. Patro, T. U.; Harikishan, G.; Mishra, A.; Evang, V. Polym Eng and Sci 2008, 48, 1178.
30. Zhang, Y.; Han, W.; Liu, W.; Aixu, S.; Feiwu, C. J Macromol Sci 2008, 47, 532.
31. Valle, V. R.; Lerf, A.; Wanger, F. E.; Poyato, J.; Rodriguez, J. L. P.; J Thermal Anal Cal 2008, 92, 43.
32. Tang, Z.; Lu, D. Guo, J.; Su, Z; Mat Lett, 62 2008, 26, 4223.
33. Mittal, V. J Comp Matl 2008, 42, 2829.
34. Scarber, R. UAB Mc Nair; Chronicle 2005, 90, 27.
35. Yang, J. P.; Yang, G.; Xu, G.; Fu, S. Y. Comp Sci Tech 2007, 67, 2934.
36. Ke, Y. C.; Stroeve, P. Polymer-Layered Silicate and Silica Nanocomposites; Elsevier BV: Amsterdam, Netherlands, 2005.
37. Mondal, M.; Chattopadhyay, P. K.; Chattopadhyay, S.; Setua, D. K. Thermochimica Acta 2010, 510, 185.
38. Mondal, M.; Chattopadhyay, P. K.; Setua, D. K.; Das, N. C.; Chattopadhyay, S. Adv Mat Res 2010, 435, 123–125.
39. Mondal, M.; Chattopadhyay, P. K.; Setua, D. K.; Das, N. C.; Chattopadhyay, S. Polym Intl to appear.
40. Tian, M.; Cheng, L.; Liang, W.; Zhang, L.; Macromol Mater Eng 2005, 290, 681.
41. Khan, S. U.; Iqbal, K.; Munir, A.; Kim, J.-K. Compos Part A Appl Sci Mafac; 2011, 42, 253.
42. Kroshefsky, R. D.; Price, J. L.; Mangaraj, D.; Rubber Chem Technol; 2009, 82, 340.